

CHAPTER III

PRESSURE DEPENDENCE OF THE SMECTIC A LAYER SPACING OF 4'-n-OCTYLOXY-4-CYANOBIIPHENYL IN RELATION TO ITS RE-ENTRANT BEHAVIOUR

3.1 Introduction

As already mentioned in chapter I, Gladis¹ discovered that binary mixtures of p-[p-hexyloxy-benzylidene)-amino]benzotrile (HBAB) and N-p-cyano-benzylidene-p-n-octyloxyaniline (CBOOA) exhibit the following interesting sequence of phase transitions on cooling:

isotropic \rightarrow nematic \rightarrow smectic A \rightarrow nematic \rightarrow solid.

The second nematic phase, which occurs at a lower temperature than the smectic A phase is called the 're-entrant nematic phase' in analogy to similar phases which have been observed in superconductors² and He³ (see ref. 3). It was found that as far as the macroscopic properties are concerned, there is no

difference between the two nematic phases. Subsequently, Gladis et al.⁴ discovered that a re-entrant transition is induced under elevated pressures in a pure compound, viz., 4'-n-octyloxy-4-cyanobiphenyl (8 OCB). The compound exhibits a re-entrant nematic phase in the pressure range of 1.6 to 1.8 kbar, on cooling the sample from the smectic phase. In addition, Gladis et al.^{4,5} have also discovered re-entrant nematic phases under elevated pressures in CBOOA and in mixtures of HBAB and CBOOA and also in mixtures of n-p-cyanobenzylidene-p-nonylaniline (CBNA) and n-p-cyanobenzylidene-p-heptylaniline (CBHA).

All the compounds showing the re-entrant behaviour have the highly polar cyano group attached to one end of the molecule. For such compounds, Madhusudana and Chandrasekhar⁶ have shown that the near neighbour correlations should be antiparallel. The layer spacing determinations⁷⁻⁹ in the smectic A phase for the compounds with a terminal cyano group gave a value which is nearly 1.4 times the molecular length. This appears to be a characteristic feature of the compounds which possess

the polar cyano group at one end and the non polar aliphatic tail at the other end. These experimental results could be explained if the molecules in the smectic A phase have some sort of interdigitation and form a bilayer structure.

In the bilayer smectic model proposed,^{4,9,10} the cyano-aromatic segments (called the polar part) overlap. The aliphatic chains (called the non polar part) extend outwards. This model fits the measured layer spacings which are never commensurate with the molecular length. The antiparallel ordering between the neighbouring molecules in the bilayer smectic A is now confirmed experimentally by Leadbetter et al.¹¹ from neutron scattering studies.

According to Gladis et al.,⁴ in a smectic A bilayer, the forces stabilising the layers are the short range attractive hydrocarbon (nonpolar-nonpolar) interactions. The interactions of the aromatic groups (polar-polar) becomes repulsive when pressure is applied. At higher pressures, the strong repulsive force

resisting the compression, drives the layers apart (Fig. 3.1). Hence, by assuming that the polar-polar and non polar-non polar interactions must be maintained to ensure the stability of the bilayer smectic A, Gladis et al. proposed that the layer spacing expands with increasing pressure.

Soon after the discovery of the high pressure re-entrant phenomenon in 8 OCB, we undertook a high pressure X-ray study of the pressure dependence of the smectic A layer spacing in 8 OCB using the diamond anvil cell described in the previous chapter. Preliminary results appeared to indicate that the layer spacing does indeed expand with increase in pressure beyond about 1.6 kbar.¹² Guillon et al.¹³ also carried out some preliminary studies, but did not report any details of their findings. We refined our experimental technique to a much greater precision and have subsequently been able to confirm for the first time the validity of Gladis' prediction.

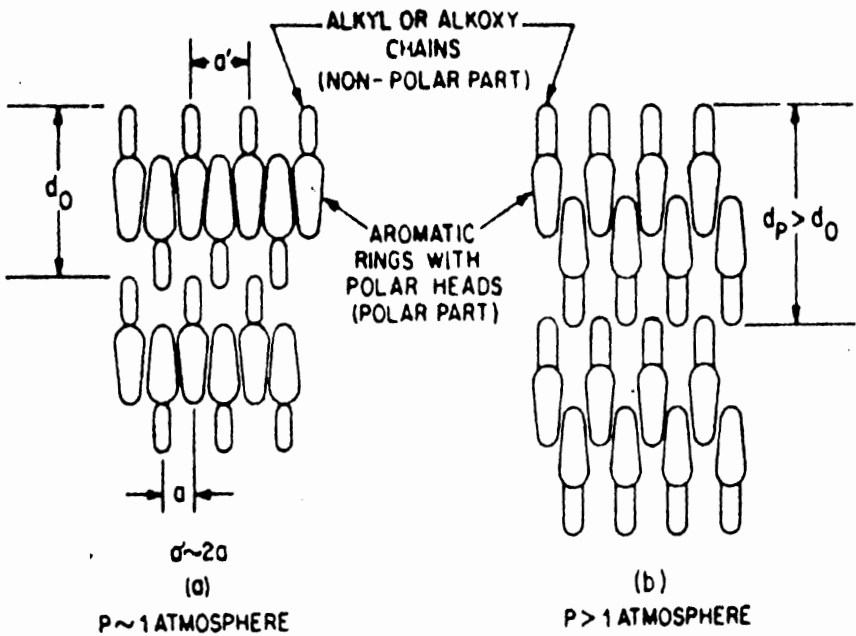


Figure 3.1

Schematic diagram of a bilayer smectic A phase at (a) 1 atmosphere, and (b) under pressure. (After Gladis et al.⁴).

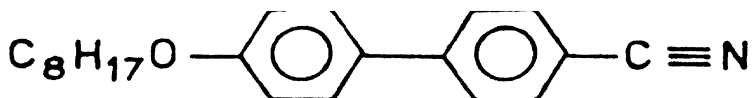
3.2 Experimental

a) Compound. The sample 8 OCB used in our experiments was obtained from BDH, England. The molecular structure of the compound is given in figure 3.2. The transition temperatures at atmospheric pressure were determined by using a polarising microscope used in conjunction with a Mettler FP52 hot stage and FP5 temperature controller. They are,

solid $\xrightarrow{54.5^{\circ}\text{C}}$ smectic A $\xrightarrow{66.9^{\circ}\text{C}}$ nematic $\xrightarrow{80^{\circ}\text{C}}$ isotropic.

These values agree with those reported by Cladis et al. Hence the P-T diagram of 8 OCB obtained by Cladis et al.⁴ was used in our experiments for the determination of pressure, after the 'in situ' optical determination of the transition temperature of the sample in the cell.

b) Phase diagram of 8 OCB. The P-T diagram of 8 OCB, obtained by Cladis et al.⁴ is shown in fig. 3.3. It can be seen from the diagram that the solid-smectic A, the smectic A-nematic, and the nematic-isotropic transition temperatures increase initially as expected, with increase



4'-n-octyloxy-4-cyanobiphenyl
(8 OCB)

FIGURE 3.2

Structural formula of 8 OCB

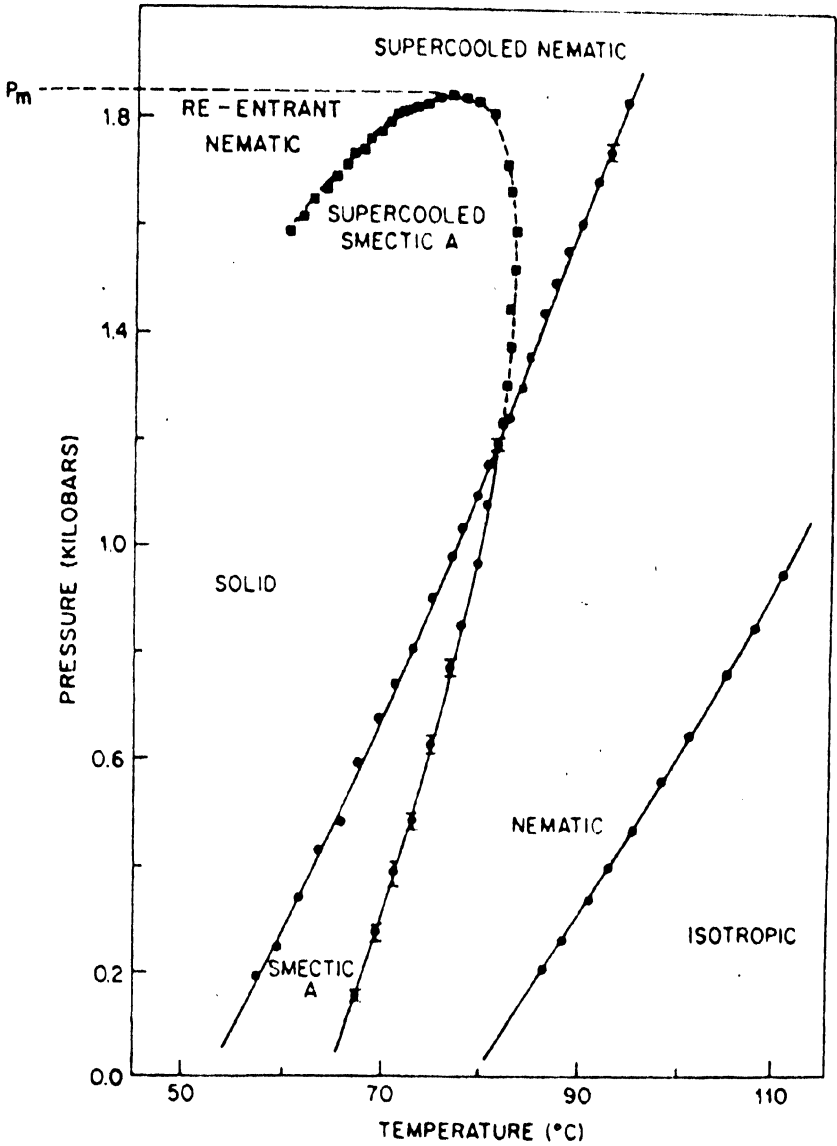


FIGURE 3.3

P-T diagram of 8 OCB. P_m is the maximum pressure at which the smectic phase exists for this compound. (After Cladis et al.⁴).

in pressure. But at higher pressures, the range of the nematic phase increases at the expense of the smectic phase. The smectic A-nematic phase boundary curves towards the pressure axis. The smectic A phase gets bounded near 82°C and at a pressure of 1.2 kbars there is a triple point with the coexistence of the solid, smectic A and the nematic phases. Thereafter, the solid directly goes over to the nematic phase on heating.

In the cooling mode, (figure 3.4), we get the interesting part of the phase diagram. Beyond pressures of 1.2 kbar, the nematic phase supercools and has a transition to the smectic A. Between the pressure range of about 1.6 to 1.8 kbar, the supercooled smectic A transforms into a nematic again at a lower temperature. This is the re-entrant nematic phase.

The dP/dT values for the smectic A-nematic phase boundary initially increase with pressure (figure 3.4). At higher pressures, the value becomes ∞ . After this, the dP/dT value becomes negative. At the maximum

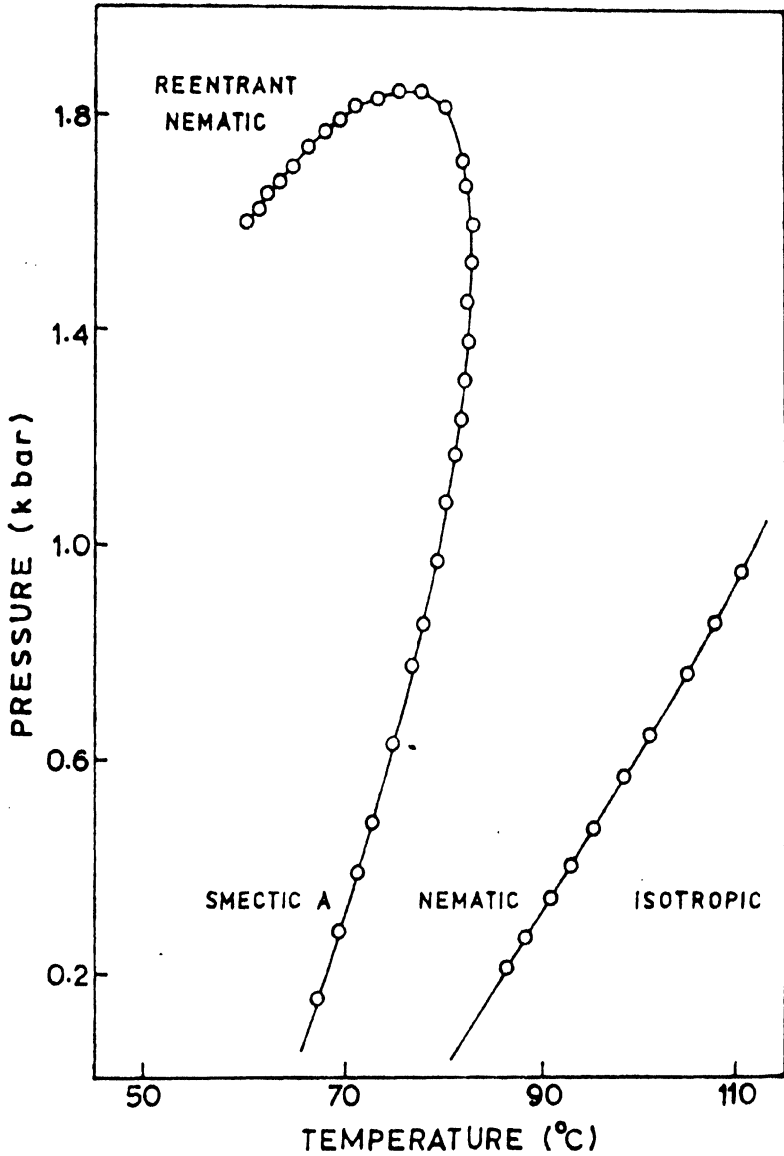


FIGURE 3.4: P-T Diagram of 8 OQB showing the isotropic nematic, smectic A and re-entrant nematic phases in the cooling mode. (After Cladis et al.⁴).

pressure (P_m) for which the smectic phase exists, $dP/dT = 0$. The value of dP/dT becomes positive again for the re-entrant region, as the boundary curves down. These phase boundary characteristics are found for all the compounds which show the re-entrant phase at elevated pressures.

c) Determination of pressure. The diamond anvil cell, described in chapter II, was used for our experiments. The 'in situ' transition temperatures of the sample in the cell were determined by the optical transmission technique discussed in section 4(a) of chapter II. For the accurate determination of the pressure, both the solid-smectic A and smectic A-nematic transitions were found. At higher pressures, both the solid-nematic and the nematic-smectic A (in the cooling mode) transitions were used to fix the pressure. The phase transition temperatures at any pressure could be reproduced to an accuracy of $\pm 0.2^\circ\text{C}$. The accuracy of the pressure values is estimated to be ± 15 bars.

During the transition temperature determinations, there was a problem in determining the solid to smectic A transition temperature owing to the supercooling of the mesophase of the sample in the gasket. It was found that on melting a freshly filled sample, it transforms into smectic A, nematic and isotropic phases on heating. However, on cooling, the sample in the smectic A phase cooled into another crystalline phase (referred to as solid-2, S_2 phase) which was observed to be relatively transparent. In comparison, the original crystalline phase (S_1 phase) was extremely opaque. It was found that although the S_2 phase remained in that state without transforming into S_1 phase, in spite of keeping the sample at a low temperature for several hours, the $S_2 \rightarrow S_1$ transformation could be easily brought about by heating the sample in S_2 phase to S_1 phase. In all our experiments, it was ascertained that only the S_1 to smectic A transitions were determined at each pressure.

d) X-ray measurements: The X-ray diffraction maxima were recorded photographically. As the aim of the

experiment was to measure small variations in the layer spacing, the sample-to-film distance was kept quite large (approximately 290 mm). Usually, with the diamond anvil cell, Mo radiation is used. But, in this case, this was not preferred because the diameter of the diffraction pattern obtained with the experimental set up was found to be too small. Hence Ni-filtered CuK_α radiation from a fine focus Philips tube was used despite the fact that there was large attenuation of the intensity of the X-ray beam on passage through the diamond anvils. The duration of each exposure was around ^{one} hundred hours. The temperature was maintained constant to within $\pm 0.25^\circ\text{C}$ throughout the exposure. The photograph at every pressure was taken 3°C below the normal nematic-smectic A transition point to minimise the effect of temperature on layer spacing.

A new gasket, packed with fresh sample, was used for the experiments at each exposure. Also, after the end of each exposure, the 'in-situ' transition temperatures of the sample in the cell were redetermined by the optical

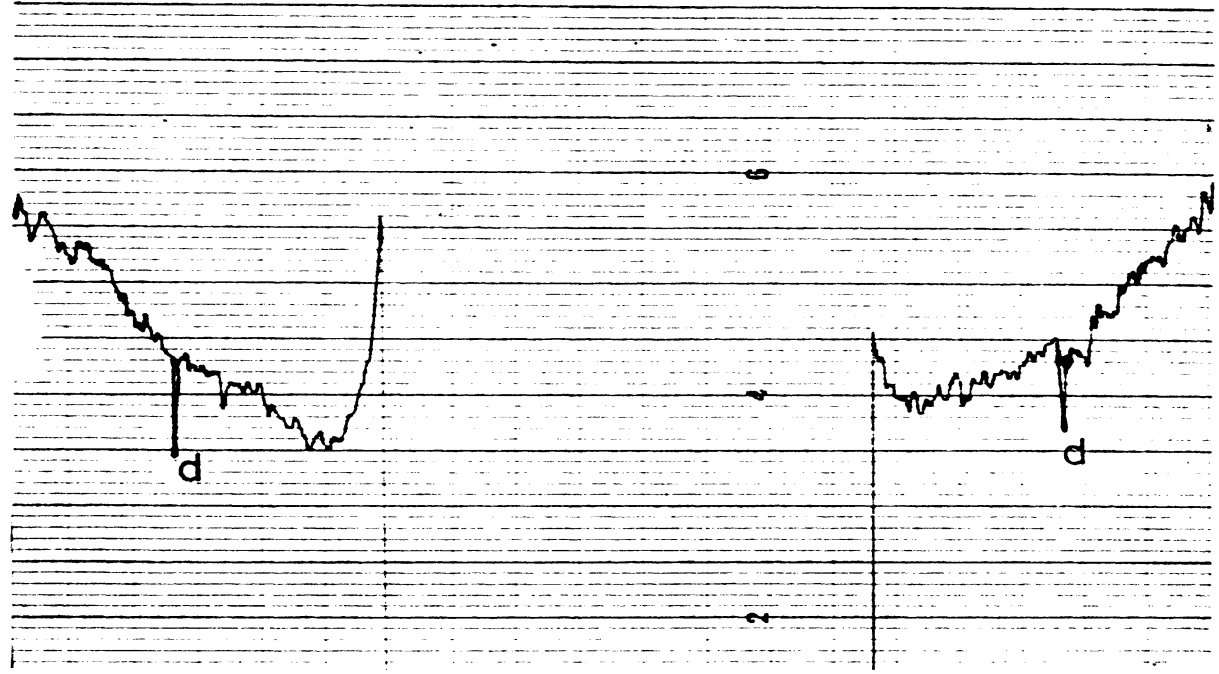
transmission technique. These were found to be exactly the same as those measured before the commencement of the exposure. This indicates that the pressure was maintained constant throughout the exposure.

The sample-to-film distance was accurately determined by using the 100 reflection ($d = 23.10 \text{ \AA}$) of p-decanoic acid.¹⁴ The indentation in the gasket and the consequent change in the sample-to-film distance was found to be less than 0.2 mm even at the highest pressure and was therefore neglected compared to the large sample-to-film distance (about 290 mm).

The diameters of the diffraction rings were measured by using microdensitometer (Carl-Zeiss Model II) traces of the X-ray photographs. A typical raw densitometer trace is shown in figure 3.5. For all photographs, the chart speed and the scanning rate were chosen to give a magnification of 5. The peak-to-peak distance (P to P in the figure 3.5) measured with an accurate comparator (Adam Hilger Ltd., London) was used to evaluate the layer spacing.

Raw densitometer trace of the x-ray photograph. P is the diffraction peak. While taking the trace the source of light is turned off near the beam stopper position.

FIGURE 3.5



To ascertain that the film was normal to the incident beam, the diffraction ring of each photograph was scanned along different diameters. The peak-to-peak distance corresponding to each scan was measured. No systematic deviation in the peak-to-peak distance was noticed for the different scans. The internal consistency of the layer spacing evaluated from the different diameters of any one diffraction ring was found to be better than $\pm 0.1 \text{ \AA}$. It is therefore estimated that the relative accuracy of the layer spacing at different pressures is $\pm 0.1 \text{ \AA}$ or better. As mentioned earlier, the data were brought to an absolute scale by using the p-decanoic acid as the standard.

3.3 Results and Discussion

It is well known that the layer spacing is related to the diameter of the diffraction ring by the equation $2d \sin \theta = n\lambda$ where n is the order of diffraction (which is equal to 1 for our experiments), d is the layer spacing, λ the wavelength of X-rays and θ is given by the relation $\tan 2\theta = \frac{D}{2S}$ where D is the diameter of the ring and S is the sample-to-film distance. The mean ring

diameter (D) obtained by scanning each ring in three or more different directions and the layer spacing d evaluated from the D values for the different pressures for which the photographs were taken, are given in table 3.1. The data are plotted in figure 3.6.

The values obtained for the layer spacing at atmospheric pressure agree very well with the recent determinations of the same by Leadbetter et al.¹¹ and by Gladis et al.⁵ It is seen from figure 3.6 that the layer spacing decreases more or less uniformly at the rate of 0.6 \AA per kbar till the pressure attains 1.4 kbar, beyond which it increases.

The question may be asked as to what is the contribution of pure temperature variation of the layer spacing to the curve shown in figure 3.6. To find out whether there is any such thermal variation, the layer spacing of 8 OCB was measured at atmospheric pressure, at various temperatures covering the entire smectic phase using the experimental set up which will be described in chapter IV. It was found that there is no detectable change in the

TABLE 3.1

Layer spacings in the smectic A phase of 8 OCB at different pressures

Sample-to-film distance = 288.4 mm

Pressure (kbars)	Mean diameter (mm)	Layer spacing (Å)
Lab. pressure	27.80	32.00
0.22	27.91	31.89
0.41	28.03	31.76
0.61	28.14	31.63
0.90	28.37	31.38
1.08	28.42	31.32
1.35	28.50	31.23
1.48	28.38	31.36
1.52	28.41	31.33
1.62	28.26	31.50
1.69	28.17	31.60
1.72	28.14	31.63

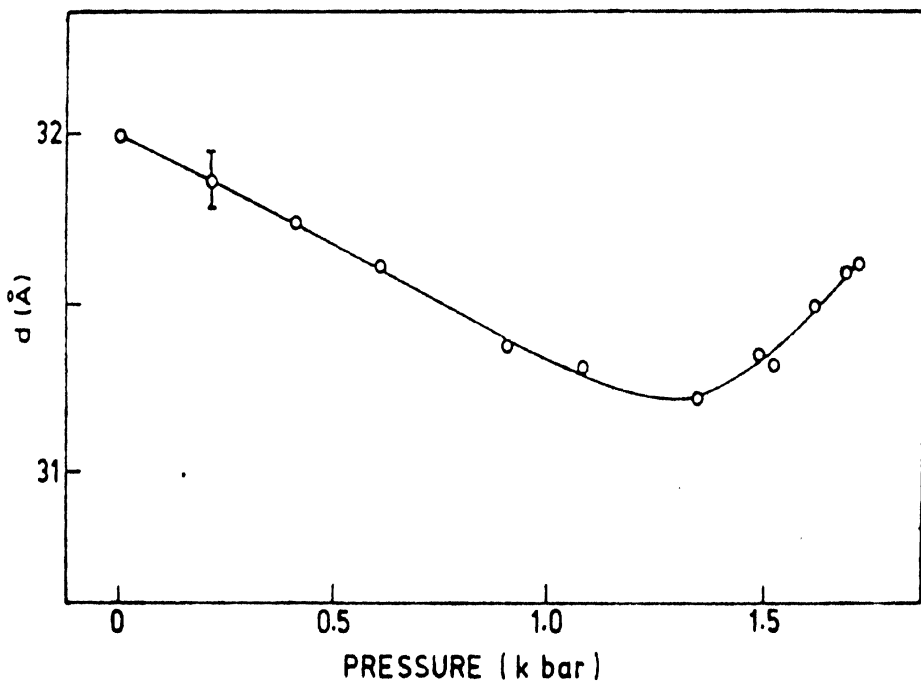


FIGURE 3.6

Plot of the smectic A layer spacing of 8 OCB versus pressure. The error bar indicates the precision of the measurements.

layer spacing with temperature within the limits of our experimental accuracy ($\pm 0.1 \text{ \AA}$).

Thus, we can conclusively say that the re-entrant behaviour of 8 OCB, which occurs at higher pressures, is associated with an expansion of the smectic A layer spacing with increase in pressure, as was indeed predicted by Gladis et al.

We may mention here the high pressure x-ray investigation on CBOOA by Guillon et al.¹⁵ CBOOA has a terminal cyano group and it exhibits the re-entrant nematic phase in the cooling mode at high pressures. In their experiment on CBOOA, Guillon et al. varied the pressure at constant temperatures. They have determined the layer spacing in the smectic A phase both at relatively high temperatures and at low temperatures as a function of pressure.

Two samples of CBOOA, one without purification and the other recrystallised thrice, were used in the experiments by Guillon et al. For the first sample it was

observed by them that (i) as the sample ages (on a time scale of days) the pressure of transition between the smectic phase and the re-entrant nematic phase increases slowly, (ii) the layer spacing in the smectic A phase increases as a function of time, (iii) the layer spacing in the smectic A phase does not change each time the re-entrant nematic phase is obtained at high pressure. The first and second features, according to Guillon et al. is due to the shift of the smectic-nematic boundary line in the (P-T) plane caused by the presence of impurity or by the degradation of sample with time.

The second sample behaved like the first for temperatures above 72°C. But for temperatures below 72°C, where the smectic A phase is compressed toward a solid phase (rather than a re-entrant nematic phase) it was found that the layer spacing decreases with increasing pressure.

Thus the smectic A layer spacing in CBOOA shows two kinds of behaviour with increasing pressure (i) A decrease in layer spacing occurs when the smectic A phase is

compressed towards the stable solid transition. The change is small (about 1%). (ii) There is no change at all in the layer spacing when the smectic A phase is compressed toward the re-entrant nematic phase.

Our study on the pressure variation of smectic A layer spacing in 8 OCB is at a constant relative temperature with respect to the nematic-smectic A phase boundary whereas the study on CBOOA is at different pressures keeping the temperature constant. In our studies, the transition temperatures of the sample used were checked after each exposure, at atmospheric pressure, to detect any decomposition of the compound. It was found that the transition temperatures did not change from their initial values, proving thereby that the sample did not undergo any decomposition.

Since the experimental conditions in the two studies are different, a direct comparison of our results with the results obtained by Guillon et al. is not easily possible.

References

- 1 P.E.Cladis, Phys. Rev. Lett., 35, 48 (1975).
- 2 P.Schlottman, J.Low Temp.Phys., 20, 123 (1975).
- 3 A.C.Anderson, W.Reese and J.C.Wheatly, Phys.Rev. 130, 164 (1963).
- 4 P.E.Cladis, R.K.Bogardus, W.B.Daniels and G.N.Taylor, Phys. Rev. Lett., 39, 720 (1977).
- 5 P.E.Cladis, R.K.Bogardus and D.Aadsen, Phys. Rev., A18, 2292 (1978).
- 6 N.V.Madhusudana and S.Chandrasekhar, Proceedings of the International Liquid Crystals Conference, Bangalore, 1973 - Pramana Supplement 1, p.57. Also N.V.Madhusudana, K.L.Savithramma and S.Chandrasekhar, Pramana, 8, 22 (1977).
- 7 W.L.McMillan, Phys. Rev., A7, 1419 (1973).
- 8 G.W.Gray and J.E.Lydon, Nature, 252, 221 (1974) Also, J.E.Lydon and C.J.Coakley, J.Phys.(Paris), 36, C1-45 (1975).
- 9 A.J.Leadbetter, R.M.Richardson, C.N.Colling, J.Phys. (Paris), 36, C1-37 (1975).
- 10 A.J.Leadbetter, J.L.A.Durrant and M.Rugman, Mol. Cryst. Liq. Cryst. 34, 231 (1977).
- 11 A.J.Leadbetter, J.C.Frost, J.P.Gaughan, G.W.Gray and A.Mosley, J. Phys. (Paris), 40, 375 (1979).
- 12 S.Chandrasekhar, University Lecture delivered at Birkbeck College, London on 31 October 1977. Summary published in Curr. Sci., 47, 523 (1978).

- 13 D. Guillon, D.R.Aadsen, P.E.Cladis, J.Stamatoff and W.B.Daniels, Abstract, VII International Liquid Crystals Conference, Bordeaux, July 1978.
- 14 D. Guillon and P.E.Cladis (private communication).
- 15 D. Guillon, P.E.Cladis, D. Aadsen, and W.B.Daniels, Phys. Rev. A21, 658 (1980).